Am J Cancer Res 2021;11(4):1616-1631
www.ajcr.us /ISSN:2156-6976/ajcr0127466

Original Article

Concurrence of Myelodysplastic syndromes and large granular lymphocyte leukemia: clinicopathological features, mutational profile and gene ontology analysis in a single center

Kexin Ai[1,2*], Minming Li[2*], Ping Wu[2], Chengxin Deng[2], Xin Huang[2], Wei Ling[2], Ruohao Xu[2], Suxia Geng[2], Qihui Sun[2], Jianyu Weng[2], Xin Du[1,2]

[1]The Second School of Clinical Medicine, Southern Medical University, Guangzhou 510515, Guangdong, P. R. China; [2]Department of Hematology, Guangdong Provincial People's Hospital, Guangdong Academy of Medical Sciences, Guangzhou 510080, Guangdong, P. R. China. [*]Equal contributors.

Received December 2, 2020; Accepted February 4, 2021; Epub April 15, 2021; Published April 30, 2021

Abstract: The concurrence of Myelodysplastic syndromes (MDS) and large granular lymphocyte leukemia (LGLL) has been reported in a small group of patients and might suggest an etiologic relationship rather than a simple coincidence. In this present study, clinicopathological features were detailed in ten cases of MDS concurrent with LGLL (MDS-LGLL). These cases included seven patients with T-LGLL, two with mixed-phenotype LGLL, and one with CLPD-NK. Subsequently, gene mutation screening for commonly myeloid-related or lymphoid-related genes was performed in MDS-LGLL patients by using next generation sequencing (NGS). The genes with the highest frequency of mutations were *ASXL1* (3/10, 30%) and *STAG2* (3/10, 30%) among a panel of 114 genes. LGLL-associated mutations of *STAT3* (2/10, 20%) and *STAT5b* (1/10, 10%) were also detected. Moreover, whole-exome sequencing (WES) and gene ontology (GO) analysis for one patient in his different phases revealed increased enrichment of histone H3 lysine 4 (H3K4) mono-methylation (GO:0097692) pathway and decreased enrichment of translocation of ZAP-70 to immunological synapse (R-HAS-202430) pathway upon progression from MDS to MDS-LGLL.

Keywords: Myelodysplastic syndromes, large granular lymphocyte leukemia, concurrence, mutational profile, gene ontology analysis

Introduction

Myelodysplastic syndromes (MDS) are a group of heterogeneous malignant hematopoietic stem cell (HSC) disorders characterized by blood cytopenia and frequently progress to acute myeloid leukemia (AML) [1]. Increasing evidences suggest that cellular immunodeficiency participates in pathogenesis of MDS [2]. Immune alterations are complex and intertwined with hematopoiesis and bone marrow (BM) microenvironment dysfunction in MDS [2]. Moreover, immunosuppressive treatment for a subgroup of MDS patients, such as antithymocyte globulin (ATG) or cyclosporine, may significantly improve anemia and neutropenia [3].

Large granular lymphocyte leukemia (LGLL) are under the categories of T and natural killer (NK) cell lymphomas and usually indole [4]. There are three subtypes of LGLL, approximately 85% of reported LGLL cases are the T-cell large granular lymphocyte leukemia (T-LGLL) subtype, 10% of cases described as Chronic lymphoproliferative disorder of NK-cells (CLPD-NK) and the last 5% are aggressive NK-cell leukemia [5, 6]. T-LGLL and CLPD-NK exhibit similar clinical and biologic pattern, but different immunophenotype. Generally, T-LGLL cells exhibit a mature post-thymic phenotype, mostly displaying CD3+, CD4-, CD5dim, CD8+, CD16+, CD27-, CD28-, CD45RA+, CD57+ and TCRαβ+; whereas CLPD-NK cells feature CD2+, CD3-, CD4-, CD8+, CD16+, CD56+, CD94+ and TCRαβ- [7].

A small part of patients have been reported with MDS concurrent with LGLL (MDS-LGLL)

over the past decades [8-10]. Lower hemoglobin level and erythroid dysplasia are more common in patients with MDS-LGLL comparing with MDS patients [8, 9]. However, limited data have been collected on the genetic defects of MDS-LGLL patients as Next-generation sequencing (NGS) and Whole-exome sequencing (WES) to detect pathogenic mutations were not widely used until last decade [11]. Herein, we not only described the clinicopathologic, immunophenotypic features of MDS-LGLL cases, but also analyzed the genetic mutations by NGS, WES and Gene ontology (GO) analysis.

Materials and methods

Patients

A total of 42 adult MDS patients with a possible concurrence of LGLL were identified from 721 patients diagnosed with MDS in Guangdong Provincial People's Hospital between January 2015 and December 2019. In the end, 10 patients were confirmed with MDS-LGLL based on the review of clinical records, results of bone marrow morphologic examination, immunophenotype, immunohistochemistry and TCR gene rearrangements (**Table 1**) [1, 4]. All study participants provided informed consent form in accordance with the Declaration of Helsinki and the research was approved by the ethics committee of the Guangdong general hospital (NO. GDREC2015167H).

Flow cytometry analysis

Flow cytometric analysis specifically detected CD2, CD3, CD4, CD5, CD7, CD8, CD16, CD27, CD28, CD45RA, CD56, CD57, CD94, NKG2A, NKG2C, CD158a, CD158b, CD158e, TCRαβ and TCRγδ and carried out on peripheral blood (PB) samples via standard methods. Data were collected using the FACS flow cytometer (BD Biosciences, Sunnyvale, CA, USA) and analyzed by Flowjo 10 software. We assessed Vβ TCR cell surface protein repertoire to identify clonality of T-LGL cells. The expression of a single KIR antigen (CD158a, CD158b, or CD158e) is used as acknowledged indicator of clonality of NK-LGL cells [12].

T cell receptor gene rearrangement analysis

We extracted total cellular DNA and carried out the PCR amplification with Biomed-2 primers targeting TCRb, TCRg, TCRd [13]. The clonality of the PCR product is processed via heteroduplex analysis and Gene Scanning analysis.

Next-generation sequencing

The NGS was applied using DNA extracted from BM mononuclear cells. The experiment was run under the condition of the mean depth as 170-fold. Sanger sequencing was employed to confirm the regions of low quality. Based on the prior implication in the pathogenesis of myeloid and lymphoid disease on the Blood Website, 114 genes were selected and targeted with In-Silico coverage of 100% (Table S1).

Bone marrow biopsy and immunohistochemistry

A bone marrow biopsy was necessary when the count of LGLs in PB is insufficient to diagnose [12]. We performed Immunohistochemical stains of bone marrow biopsies from MDS-LGLL patients for CD3, CD8, CD57, CD16, CD56 and Granzyme B (GzB) using methods previously described [8].

Diagnostic criteria for MDS-LGLL

According to morphological evidence, blood test, flow cytometry, karyotype or molecular genetics [14], patients with MDS were diagnosed and classified on the basis of the 2016 WHO criteria and the revised International Prognostic Scoring System (IPSS-R) [1, 15].

In order to diagnose LGLL, the immunophenotypically distinct population of each patient should fit the diagnostic criteria of T-LGLL or CLPD-NK. According to preceding studies, the diagnose of T-LGLL need meet at least 3 of the 4 criteria as follows [16, 17]: (1) T cells express complete/partial loss of one or more pan-T-cell antigens (CD2, CD5, CD7) and co-expression of one or more NK-cell antigens (CD16, CD56, CD57, CD94, NKG2A); (2) Identification of T-cell clonality by TCRvb or TCR gene rearrangement; (3) Infiltration of cytotoxic T-cell in bone marrow; (4) Persistence of the abnormal T-cell population or unexplained cytopenia for more than 6 months. Likewise, the diagnose of CLPD-NK require at least 3 of the 4 criteria as follows: (1) Loss of CD2, CD7, or CD56 in NK cells; (2) Identification of NK-cell clonality by restricted or absent expres-

Table 1. Clinical features and laboratory findings of patients with Myelodysplastic syndromes concurrent with Large granular lymphocytic leukemia (MDS-LGLL)

Patient Case No.	Age (y) and sex	Hemoglobin (g/L)	ANC ($\times 10^9$/L)	PLT ($\times 10^9$/L)	ALC ($\times 10^9$/L)	LGL count ($\times 10^9$/L)	Cell lineage Dysplasia	MDS Diagnosis	IPSS-R	Cytogenetics
1	65/Female	53	1.88	8	1.61	0.72	E, G	MDS-MLD	Intermediate	Good
2	54/Male	105	0.65	145	9.25	4.96	E, G, M	MDS-MLD	Low	Good
3	33/Female	50	2.11	259	4.47	1.30	E, M	MDS-EB-2	High	Good
4	68/Male	50	1.16	64	1.65	0.08	E, G	MDS-EB-2	High	Good
5	50/Female	74	0.20	284	1.13	0.11	E, G, M	MDS-EB-2	High	Intermediate
6	71/Male	56	1.07	17	0.85	0.35	E, G	MDS-MLD	Intermediate	Good
7	79/Female	75	0.71	163	1.13	0.34	E, G	MDS-U	Intermediate	Good
8	47/Male	75	0.93	48	1.3	0.35	E, M	MDS-MLD	Intermediate	Intermediate
9	74/Male	80	0.81	264	2.65	1.03	E, M	MDS-RS-MLD	Low	Good
10	60/Female	75	0.72	99	1.50	0.54	E, G	MDS-MLD	Intermediate	Good

E, erythroid; G, granulocyte; M, megakaryocyte.

Table 2. Morphologic features, immunophenotype, immunohistochemistry and molecular analysis of patients with myelodysplastic syndromes concurrent with large granular lymphocytic leukemia (MDS-LGLL)

Case No.	PB-LGL (%)	BM-Lym (%)	CD3+CD57+ (%)	CD3-CD16+ CD56+ (%)	Flow cytometric Findings	Immunohistochemical Findings	Clonal TCR by PCR
1	45	19	41.73	2.57	CD3+, CD8+, CD4-, CD2+, CD7-, CD5dim, CD56-, CD16-, CD57+, TCRα/β+	CD3+, CD8++, CD57++, GzB++	+ (TCRβ)
2	25	20.5	53.6	0.04	CD2+, CD3+, CD5dim, CD7dim, CD11c+, CD16+, CD57+, TCRα/β+, TCRvβ7.1:97.28%	CD3+, CD8++, CD57++, GzB++	+ (TCRβ, TCRγ)
3	29	39.5	15	5.01	CD2+, CD3+, CD8+, CD4-, CD56-, CD57+, CD16-, CD7dim, CD28-, CD5+, TCRα/β+, TCRvβ14:15.45%	CD3+, CD8++, CD57+, GzB-	+ (TCRβ)
4	5	9	NA	13.71	CD3+, CD8+, CD4-, CD56-, CD16-, CD5-	CD3++, CD8++, CD57+, GzB+++	+ (TCRβ, TCRδ)
5	10	23.5	23.5	19.9	CD3+, CD4dim, CD8+, CD16-, CD56dim, CD57+, CD5+, CD2+, CD7-, CD27-, CD28-, CD69+, TCRα/β+, TCRvβ2:36.28	CD3+, CD8+, CD57+, GzB++	+ (TCRβ, TCRδ)
6	41.6	38	10.61	41.62	CD3-, CD8+, CD57-, CD56+, CD16+, CD4+, CD25+, CD69+	CD3-, CD8++, CD57+, CD16-, CD56+, GzB++	+ (TCRβ)
7	29.8	15	NA	29.41	CD3-, CD8+, CD4-, CD16+, CD56+, CD5-, CD69+, HLADR+, Restricted KIR (CD158b)	CD3-, CD8++, CD57++, CD16+++, CD56++, GzB++	+ (TCRβ, TCRγ)
8	26.8	63	15.78	1.64	CD3+, CD5dim, CD7+, CD2+, CD56dim, CD57dim, TCRα/β+, TCRγ/δdim, CD16-	NA	+ (TCRβ, TCRδ)
9	39	25	8.2	34.77	CD3-, CD16+, CD56+, CD8dim, CD7+, CD2+, CD5-, HLADR-, CD4-, CD57-NKG2C-, NKG2Adim, Restricted KIR (CD158b)	CD3-, CD8+, CD16++, CD56++, GzB+	-
10	36.2	12	36.24	7.57	CD3+, CD8+, CD57 partical, CD2+, CD7 partical, CD16-, CD56-, CD4-, CD69-, CD5+, TCRα/β+	CD3+, CD8++, CD57++, GzB-	+ (TCRγ)

NA: not available.

sion of KIRs via a flow cytometry assay; (3) Infiltration of cytotoxic NK-cell in bone marrow; (4) Persistent existence of the abnormal NK-cell population or unexplained cytopenia for more than 6 months [17].

Whole-exome sequencing (WES)

Whole exome regions were targeted and sequenced by Novaseq6000. After sorting via Samtools-1.8, removing PCR duplicates by Picard 2.19.1 and indexing by Samtools-1.8, we used GATK V3.8 to call variation, including single nucleotide substitution and short insertion/deletion (Table S2).

Gene ontology (GO) analysis and protein-protein interaction (PPI) analysis

GO pathway analyses were performed using the R package cluster profiles and Database for Annotation, Visualization, and Integrated Discovery (DAVID). These Analyses aimed to predict the potential functions in biological process (BP), molecular function (MF), and cellular component (CC). PPI analysis was applied to analyze the Mutated genes at the protein level by STRING and to visualize molecular interaction networks by Cytoscape.

Results

Clinical features and laboratory findings

The clinical features and laboratory findings of MDS-LGLL patients, five men and five women with a median age of 62.5 years, are summarized in **Table 1**. All patients had anemia at initial diagnosis, with the hemoglobin ranging from 50 to 105 g/L (reference range, 115-150 g/L) with a median of 74.5 g/L. Eight patients suffered neutropenia, the absolute neutrophil count (ANC) is from 0.20 to 2.11 × 10^9/L (reference range, 1.80-6.30 × 10^9/L, median, 0.87 × 10^9/L). Thrombocytopenia occur in five patients. The count of platelet (PLT) is from 8 to 284 × 10^9/L (reference range, 125-350 × 10^9/L, median, 122 × 10^9/L). The absolute lymphocyte count (ALC) ranged from 0.85 to 9.25 × 10^9/L (reference range, 1.10-3.20 × 10^9/L, median, 1.56 × 10^9/L). The count of absolute large granular lymphocyte (LGL) ranged from 0.08 to 4.96 × 10^9/L.

The subgroups of MDS were five patients with MDS-MLD, three MDS-EB-2, one MDS-U and one MDS-RS-MLD. Erythroid dysplasia could be observed in all the MDS-LGLL patient. Cytogenetic abnormalities only occurred in two patients: case 5 (+8, 20q-) and case 8 (+8). Ten patients with MDS-LGLL had been followed up. The OS was defined as the time from the diagnosis to the date of death from any causes or to the last follow-up. Survival analysis was conducted using the Kaplan-Meier method, and 95% confidence intervals (CIs) were estimated in comparison to a reference risk of 1.0 (Figure S1). Up to now, 7 cases (7/10, 70%) survived and 3 cases (3/10, 30%) died. The median OS was 17.5 months (95% CI 10.75-51.25) (Figure S1).

Pathologic and immunophenotypic features

The morphologic features, immunophenotype, immunohistochemistry and molecular analysis of MDS-LGLL cases are summarized in **Table 2**. These cases included seven patients with T-LGLL (Case 1, 2, 3, 4, 5, 6, 10), two with mixed-phenotype LGLL (Case 7, 8), and one with CLPD-NK (Case 9).

With cytoplasm that contains azurophilic granules, LGL cells are larger than circulating peripheral lymphocytes, which make it easy to identify on a PB smear (**Figure 2A**). The median percentage of LGL was 29.4% (range, 5%-45%) on PB smears, and lymphocytes in bone marrow biopsy specimens was 22% with a range from 9% to 63%.

An aberrant T-cell or NK-cell population was identified in each case by flow cytometry (**Table 2**). T-cells that CD3+, CD8+, CD4- were expressed in five cases, and CD5 was positive expressed in six cases, with dim intensity in three cases. Positive expression of CD7 was detected in five cases, dim in two cases and partical in one case. Five cases were TCRαβ+ and TCRγδ- and one case was TCRαβ+ and TCRγδdim+. Take case 2 for example, a distinct and clonal population of T-LGL cells was shown (CD2+, CD3+, CD5dim, CD7dim, CD8+, CD11c+, CD16+, CD38+, CD57+, TCRα/β+) TCRvβ: TCRv7.1 (97.28%) (**Figure 1A**). However, flow cytometry of case 9 showing a distinct and clonal population of NK-LGL cells (sCD3-, cCD3-, CD7+, CD56+, CD2+, CD5-, CD4-, CD8-dim, CD94+, CD158a-, CD158b+, CD158e-, NKG2C-, NKG2Adim) (**Figure 1B**). TCR Vβ analysis was performed in seven patients among which three were monoclonal expression. KIRs

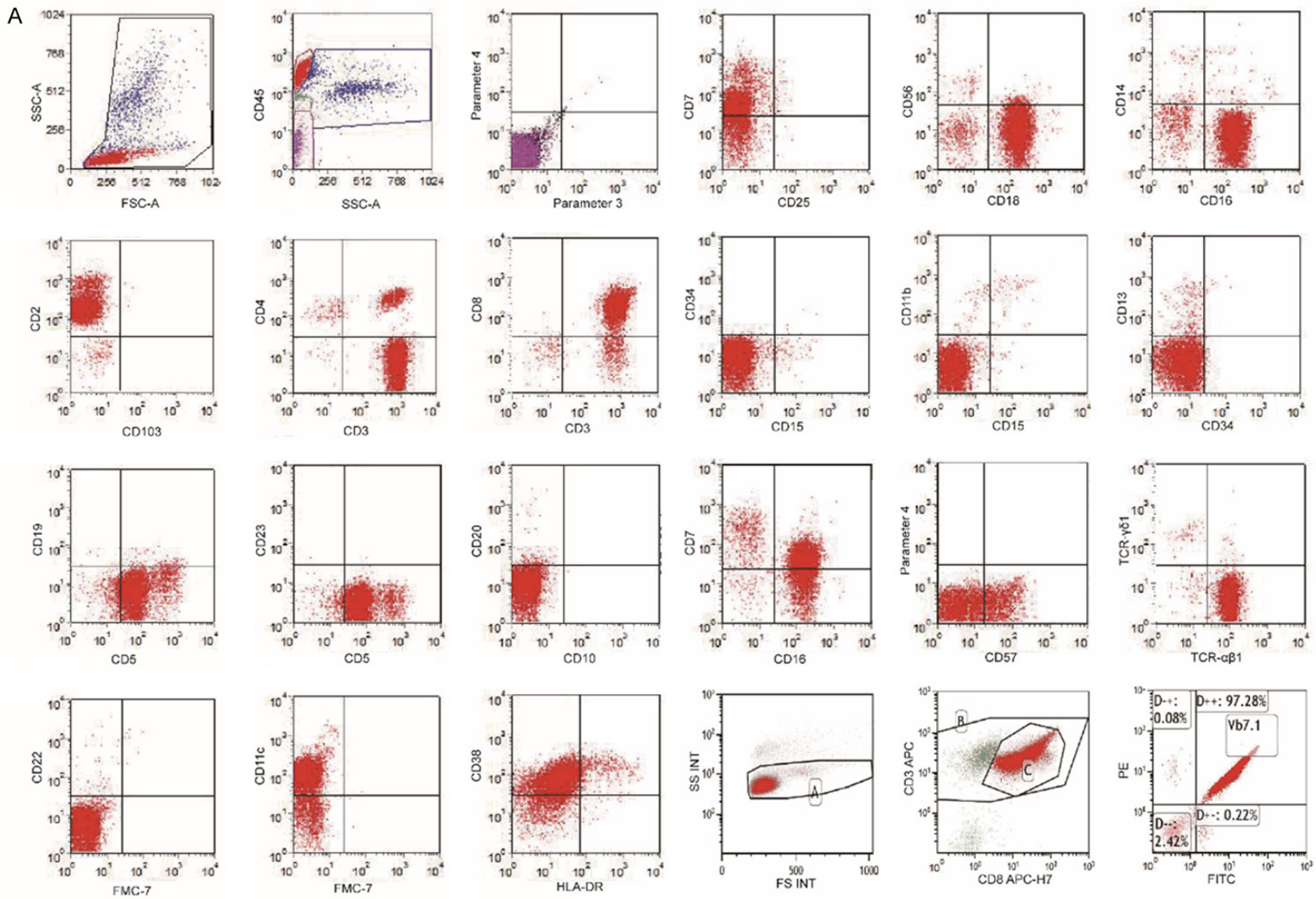
A
SSC-A
FSC-A
CD45
SSC-A
Parameter 4
Parameter 3
CD7
CD25
CD56
CD18
CD14
CD16
CD2
CD103
CD4
CD3
CD8
CD3
CD34
CD15
CD11b
CD15
CD13
CD34
CD19
CD5
CD23
CD5
CD20
CD10
CD7
CD16
Parameter 4
CD57
TCR-γδ1
TCR-αβ1
CD22
FMC-7
CD11c
FMC-7
CD38
HLA-DR
SS INT
FS INT
A
CD3 APC
CD8 APC-H7
B
C
PE
FITC
D+-: 0.08%
D++: 97.28%
Vb7.1
D--: 2.42%
D+-: 0.22%

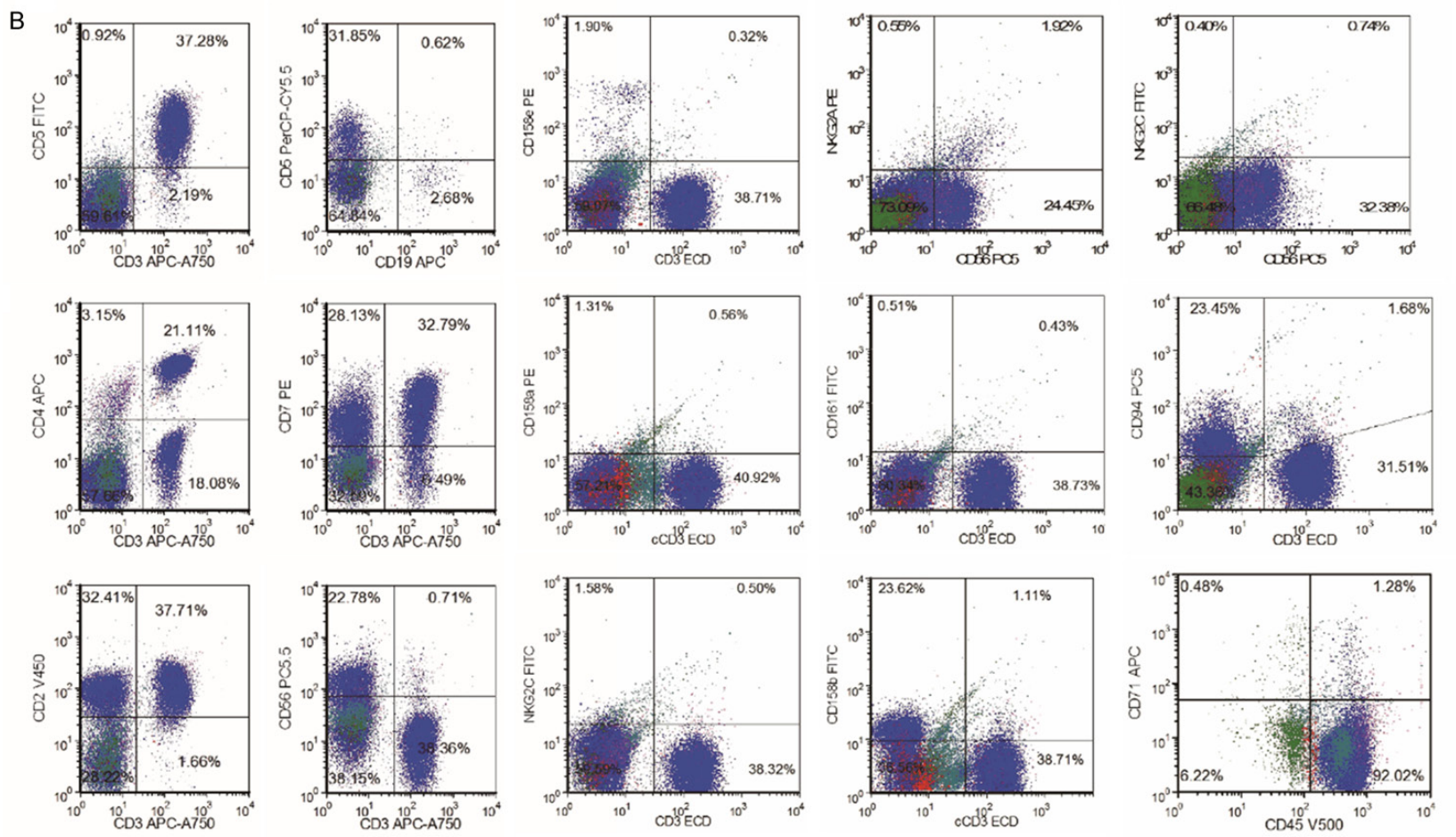

Figure 1. Flow cytometric immunophenotype of two cases of Myelodysplastic syndromes concurrent with large granular lymphocytic leukemia (MDS-LGLL). A. A distinct population of T-LGL cells showed by Flow cytometry of case 2 (CD2+, CD3+, CD5dim, CD7dim, CD8+, CD11c+, CD16+, CD38+, CD57+, TCRα/β+), TCRvb: TCRv7.1 (97.28%). B. Flow cytometry of case 9 showing a distinct population of NK-LGL cells (sCD3-, cCD3-, CD7+, CD56+, CD2+, CD5-, CD4-, CD8dim, CD94+, CD158a, CD158b+, CD158e-, NKG2C-, NKG2Adim).

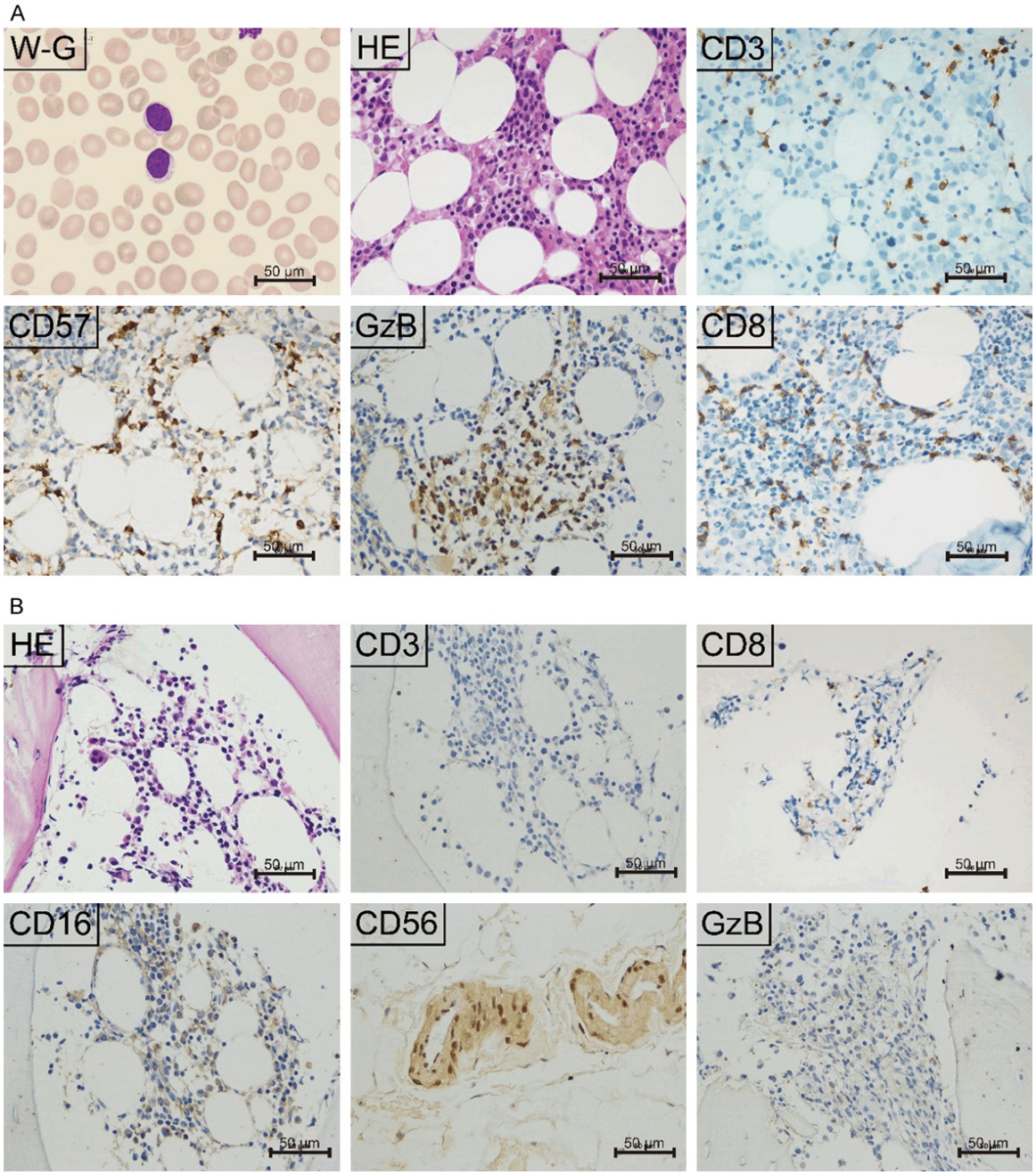

Figure 2. Representative histomorphology of two cases of Myelodysplastic syndromes concurrent with Large granular lymphocytic leukemia (MDS-LGLL). A. Interstitial lymphoid infiltrate (hematoxylin-eosin staining (HE), × 400), positive expression of CD3, CD57, Granzyme B (GzB) and CD8 by immunoperoxidase stain (× 400) in case 2. B. Bone marrow core biopsy specimens showed interstitial lymphoid infiltrate (HE, × 400), Interstitial lymphocytes are positive for CD8, CD16, CD56, GzB and negative for CD3 by immunoperoxidase stain (× 400) in case 9.

restriction (CD158b) could be identified in case 7 and case 9.

An interstitial infiltratration of CD3+ T cells was identified in six cases, CD8 and CD57 were positive in all cases by immunohistochemical analysis (**Table 2**). CD16+CD56+ NK cells were identified in two CLPD-NK cases. Granzyme B was positive in seven cases and negative in two tested cases. **Figure 2A** showed findings of Immunohistochemical stains of case 2 that diagnosed with MDS-T-LGLL. Interstitial lymphoid infiltrate (HE, × 400), positive expression of CD3, CD57, Granzyme B (GzB) and CD8 by

Table 3. Mutational profile of patients with Myelodysplastic syndromes concurrent with Large granular lymphocytic leukemia (MDS-LGLL) by Next-generation sequencing (NGS)

Patient Case No.	Mutational Genes
1	*STAT3, TP53, DNMT3A, ATM*
2	*FAT1, SETBP1, ASXL1, FLT3, CBL, GATA2, STAT3, PAX5, PTEN, SH2B3, TNFAIP3, ANKRD26, CDC25C, DIS3*
3	*CEBPA, WT1, STAG2, TP53, ATG2B*
4	*U2AF1, ASXL1, STAG2, EZH2, KIT, NOTCH1*
5	*DIS3, STAT5B, DDX41, PRDM1*
6	*DDX41, CUX1, EZH2, CSF3R, FAT1, RELN*
7	*RUNX1*
8	*TIN, ZMYM3*
9	*STAG2, TIN, ATM, PTPRT, MUC16*
10	*ASXL1, U2AF1, TET2*

immunoperoxidase stain (× 400). Moreover, patient 9, diagnosed with MDS-CLPD-NK, bone marrow core biopsy specimens showed interstitial lymphoid infiltrate (HE, × 400), Interstitial lymphocytes are positive for CD8, CD16, CD56, GzB and negative for CD3 by immunoperoxidase stain (× 400) (**Figure 2B**).

All patients exhibited TCRβ and/or TCRγ gene rearrangements by TCR gene rearrangement analysis, with the exception of case 9 that diagnosed with MDS-CLPD-NK (**Table 2**).

Gene mutations analyses by NGS

We sequenced 114 genes across ten patients with MDS-LGLL by NGS and oncogenic mutations were identified in 37 genes (**Table 3**). The histone modification *ASXL1* (3/10, 30%) and cohesin complex *STAG2* (3/10, 30%) were the most frequently mutated genes in the panel, followed by *ATM* (2/10, 20%), *STAT3* (2/10, 20%), *TP53* (2/10, 20%), *U2AF1* (2/10, 20%), *EZH2* (2/10, 20%), *DDX41* (2/10, 20%), *TIN* (2/10, 20%), *FAT1* (2/10, 20%) and *DIS3* (2/10, 20%) (**Figure 3**). The mutation rates of *STAT5b, CUX1, SH2B3, TET2, DNMT3A, SETBP1, FLT3, CBL, GATA2, PAX5, PTEN, TNFAIP3, ANKRD26, CDC25C, PTPRT, MUC16, KIT, NOTCH1, PRDM1, CSF3R, RELN, CEBPA, WT1, ATG2B and ZMYM3* were 10% (1/10). More than 3 mutated genes could be detected in eight patients.

GO pathway enrichment and PPI network analyses

GO pathway analyses were conducted to explore the underlying pathways and biological processes in MDS-LGLL of the mutated genes from two BM samples of case 2 (J9575M and Y4935) (**Figure 4**). J9575M was detected 1045 mutated genes and was collected at 2015-01-04 while the diagnosis of patient was MDS-MLD. 1044 mutated genes were detected in Y4935 which was collected at 2019-03-27 when the patient was diagnosed with MDS-LGLL. **Figure 4A** showed the top 20 pathways significantly enriched in molecular function (MF), biological process (BP) and cellular component (CC) of mutated genes. Mutated genes were found to mainly concentrate in structural constituent of epidermis in J9575M and extracellular matrix structural constituent in Y4935 In the MF group, keratinocyte differentiation in in J9575M and keratinization in Y4935 in the BP group. In the CC group, keratin filament in J9575M and intermediate filament in Y4935 were mainly enriched. **Figure 4B** showed hierarchical clustering analysis of the top 20 pathways with the biggest difference between mutated genes of J9575M and Y4935. As shown, the enrichment of H3K4 monomethylation (GO:0097692) significantly increased in Y4935, while the genes related to Translocation of ZAP-70 to immunological synapse (R-HAS-202430) pathway were less enriched.

A cohort of 247 mutated genes (Y4935) were filtered into the PPI network complex containing 238 nodes and 413 edges via the STRING online database (**Figure 5A**). **Figure 5B** summarizes three significant modules from the PPI network complex for further analysis via Cytoscape MCODE. Function annotation clusterings manifest clear association of Cluster 1 with cytokeratin pathway, Cluster 2 with mucins function, and complicated interaction in Cluster

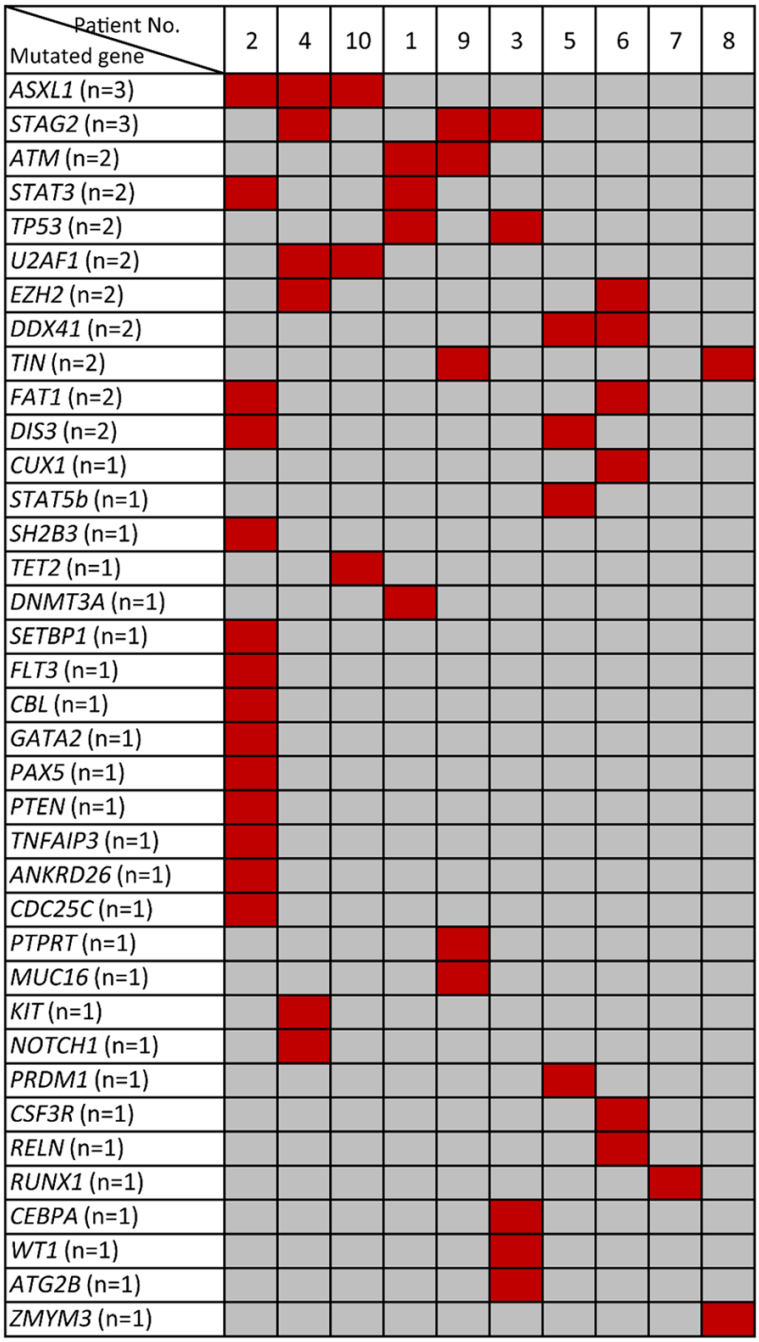

Figure 3. Distribution of mutations identified by next generation sequencing in Myelodysplastic syndromes concurrent with Large granular lymphocytic leukemia (MDS-LGLL) patients.

3 among epigenetic regulation, brain development, and DNA polymerization.

Discussion

LGL expansions can be found in a number of reactive conditions, such as viral infections, autoimmune diseases, malignancy history, certain drugs or medications, post splenectomy, and post-hematopoietic stem cell transplant (HSCT) [7, 18, 19]. Reactive LGL expansions are mainly seen in PB but rarely seen in the BM infiltrate [18]. In our study, we ruled out the factors that may lead to reactive LGL proliferation. Though previous guidelines necessitate an increase of > 2.0 × 10^9/L for > 6 months in circulating LGLs to make a definitive diagnosis of LGLL [4], patients with fewer than 2.0 × 10^9/L LGLs are often seen with clonally expanded LGLs. Therefore, a more reasonable diagnosis for LGL is believed to be between 0.2-2 × 10^9/L or even below 0.2 with evidence of clonality in the LGL population and clinical or hematological features [20].

Although a part of patients had been reported with MDS concurrent with T-cell large granular lymphocyte (LGL) proliferations over the past decades [21, 22], there are 31 MDS-LGLL cases have been reported since 2001 [8, 9, 11]. Among the 31 cases, the MDS component was classified as RCMD (8/31, 25.8%), RA (7/31, 22.6%), RAEB (6/31, 19%) and others. LGL counts were above 2 × 10^9/L in 19% (6/31) of cases, 1 to 2 × 10^9/L in 19% (6/31) of cases, and less than 1 × 10^9/L in 55% (17/31) of cases. Cytogenetic abnormalities were identified in 12 of 31 (38.7%) patients with MDS-LGLL in their studies. The levels of The median hemoglobin and absolute lymphocyte in MDS-T-LGLL patients were lower than those of MDS patients ($P < 0.05$) [8]. In this present study, we described ten cases of MDS-LGLL. Similar to previous studies, MDS-MLD (5/10, 50%) was the

A

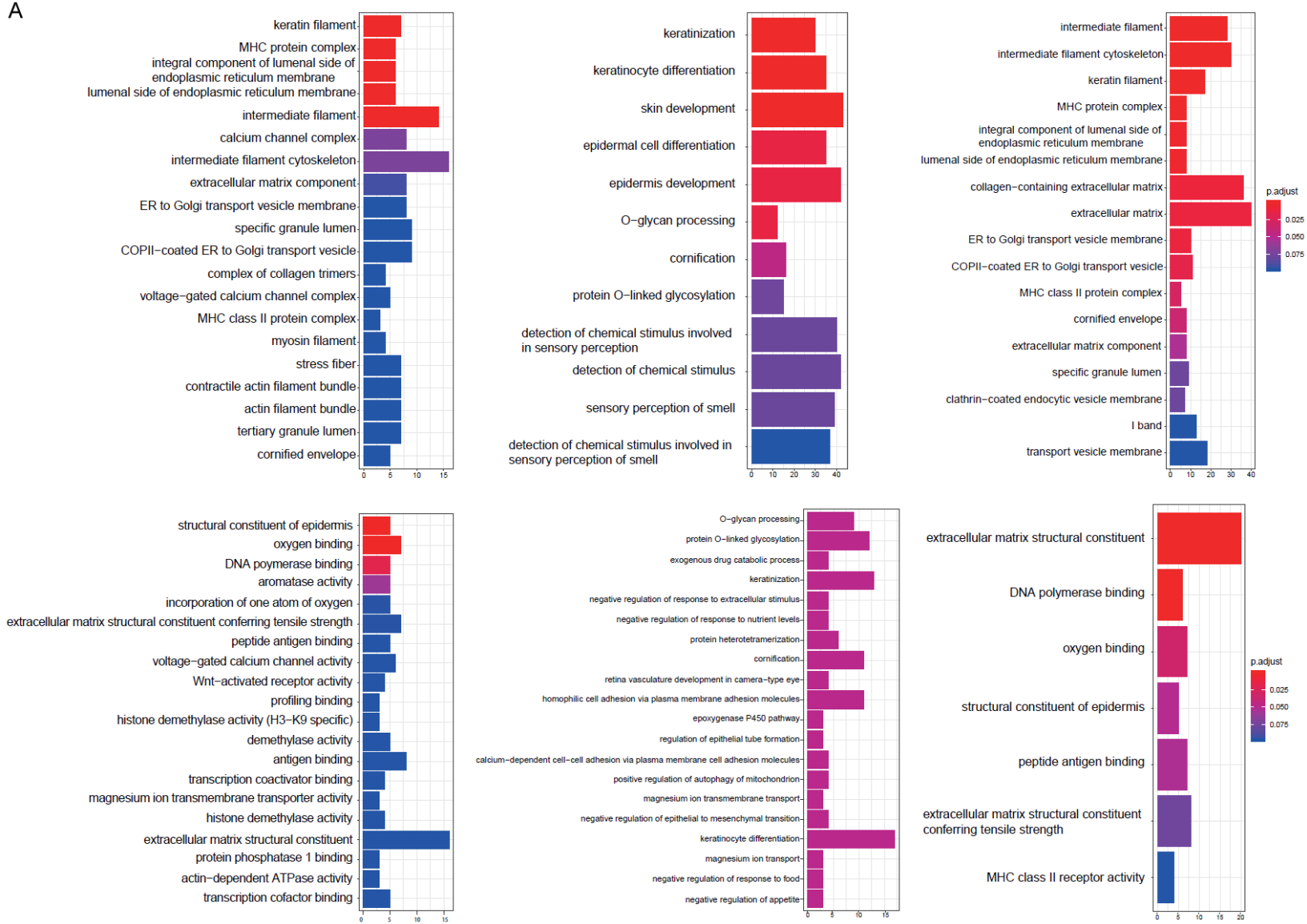
keratin filament
MHC protein complex
integral component of lumenal side of endoplasmic reticulum membrane
lumenal side of endoplasmic reticulum membrane
intermediate filament
calcium channel complex
intermediate filament cytoskeleton
extracellular matrix component
ER to Golgi transport vesicle membrane
specific granule lumen
COPII−coated ER to Golgi transport vesicle
complex of collagen trimers
voltage−gated calcium channel complex
MHC class II protein complex
myosin filament
stress fiber
contractile actin filament bundle
actin filament bundle
tertiary granule lumen
cornified envelope
keratinization
keratinocyte differentiation
skin development
epidermal cell differentiation
epidermis development
O−glycan processing
cornification
protein O−linked glycosylation
detection of chemical stimulus involved in sensory perception
detection of chemical stimulus
sensory perception of smell
detection of chemical stimulus involved in sensory perception of smell
intermediate filament
intermediate filament cytoskeleton
keratin filament
MHC protein complex
integral component of lumenal side of endoplasmic reticulum membrane
lumenal side of endoplasmic reticulum membrane
collagen−containing extracellular matrix
extracellular matrix
ER to Golgi transport vesicle membrane
COPII−coated ER to Golgi transport vesicle
MHC class II protein complex
cornified envelope
extracellular matrix component
specific granule lumen
clathrin−coated endocytic vesicle membrane
I band
transport vesicle membrane
p.adjust
0.025
0.050
0.075
structural constituent of epidermis
oxygen binding
DNA poymerase binding
aromatase activity
incorporation of one atom of oxygen
extracellular matrix structural constituent conferring tensile strength
peptide antigen binding
voltage−gated calcium channel activity
Wnt−activated receptor activity
profiling binding
histone demethylase activity (H3−K9 specific)
demethylase activity
antigen binding
transcription coactivator binding
magnesium ion transmembrane transporter activity
histone demethylase activity
extracellular matrix structural constituent
protein phosphatase 1 binding
actin−dependent ATPase activity
transcription cofactor binding
O−glycan processing
protein O−linked glycosylation
exogenous drug catabolic process
keratinization
negative regulation of response to extracellular stimulus
negative regulation of response to nutrient levels
protein heterotetramerization
cornification
retina vasculature development in camera−type eye
homophilic cell adhesion via plasma membrane adhesion molecules
epoxygenase P450 pathway
regulation of epithelial tube formation
calcium−dependent cell−cell adhesion via plasma membrane cell adhesion molecules
positive regulation of autophagy of mitochondrion
magnesium ion transmembrane transport
negative regulation of epithelial to mesenchymal transition
keratinocyte differentiation
magnesium ion transport
negative regulation of response to food
negative regulation of appetite
extracellular matrix structural constituent
DNA polymerase binding
oxygen binding
structural constituent of epidermis
peptide antigen binding
extracellular matrix structural constituent conferring tensile strength
MHC class II receptor activity
p.adjust
0.025
0.050
0.075

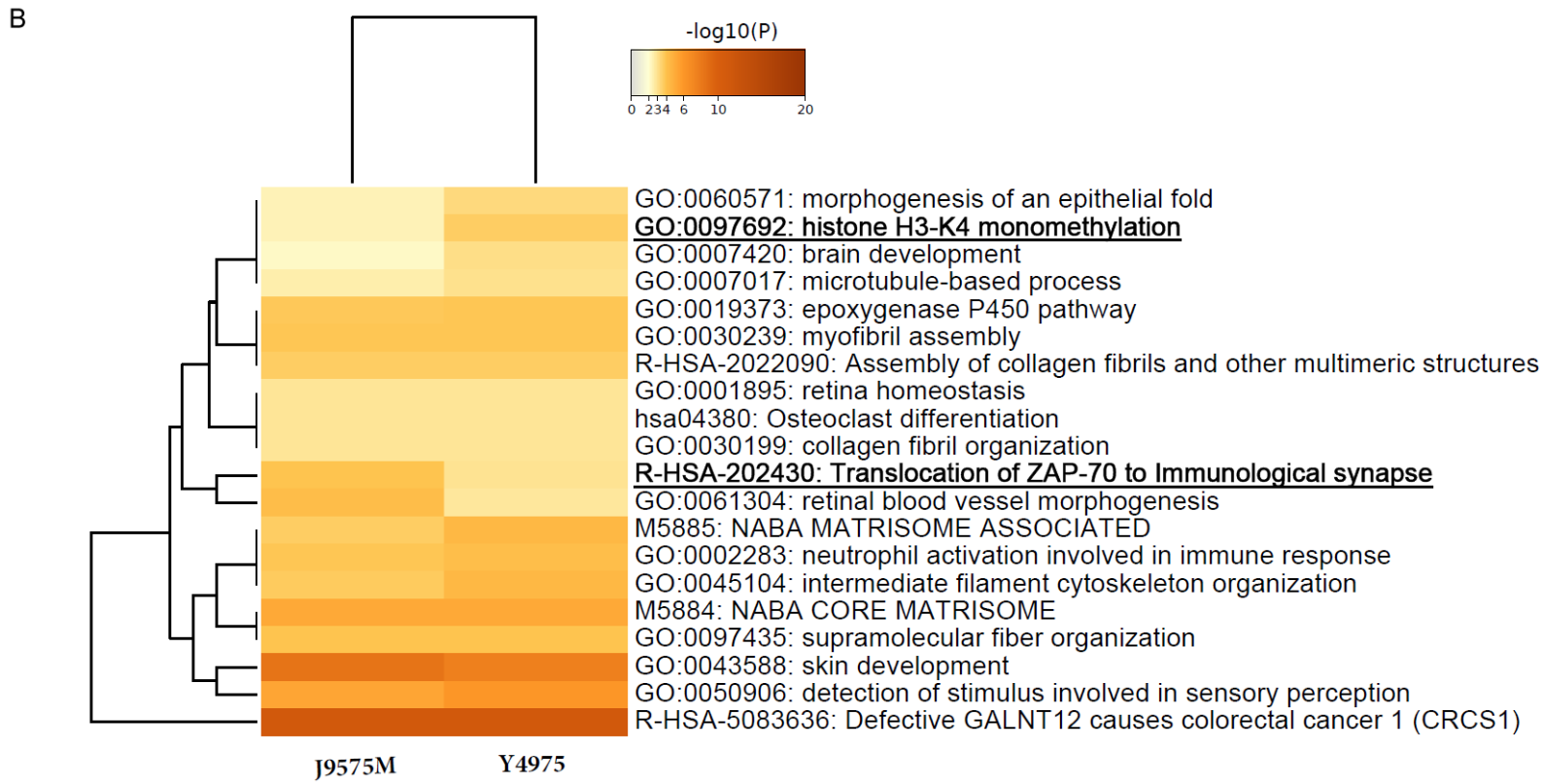

Figure 4. Gene ontology (GO) analysis and significant enriched GO terms of mutated genes in case 2. A. Top 20 pathways significantly enriched in molecular function (MF), biological process (BP) and cellular component (CC). B. Hierarchical clustering analysis of the top 20 pathways with the largest enrichment difference between J9575M and Y4935. Enrichment (-log10 (P), color bar) of these 20 pathways (rows) that are differentially expressed in each cluster (columns) can be seen.

A

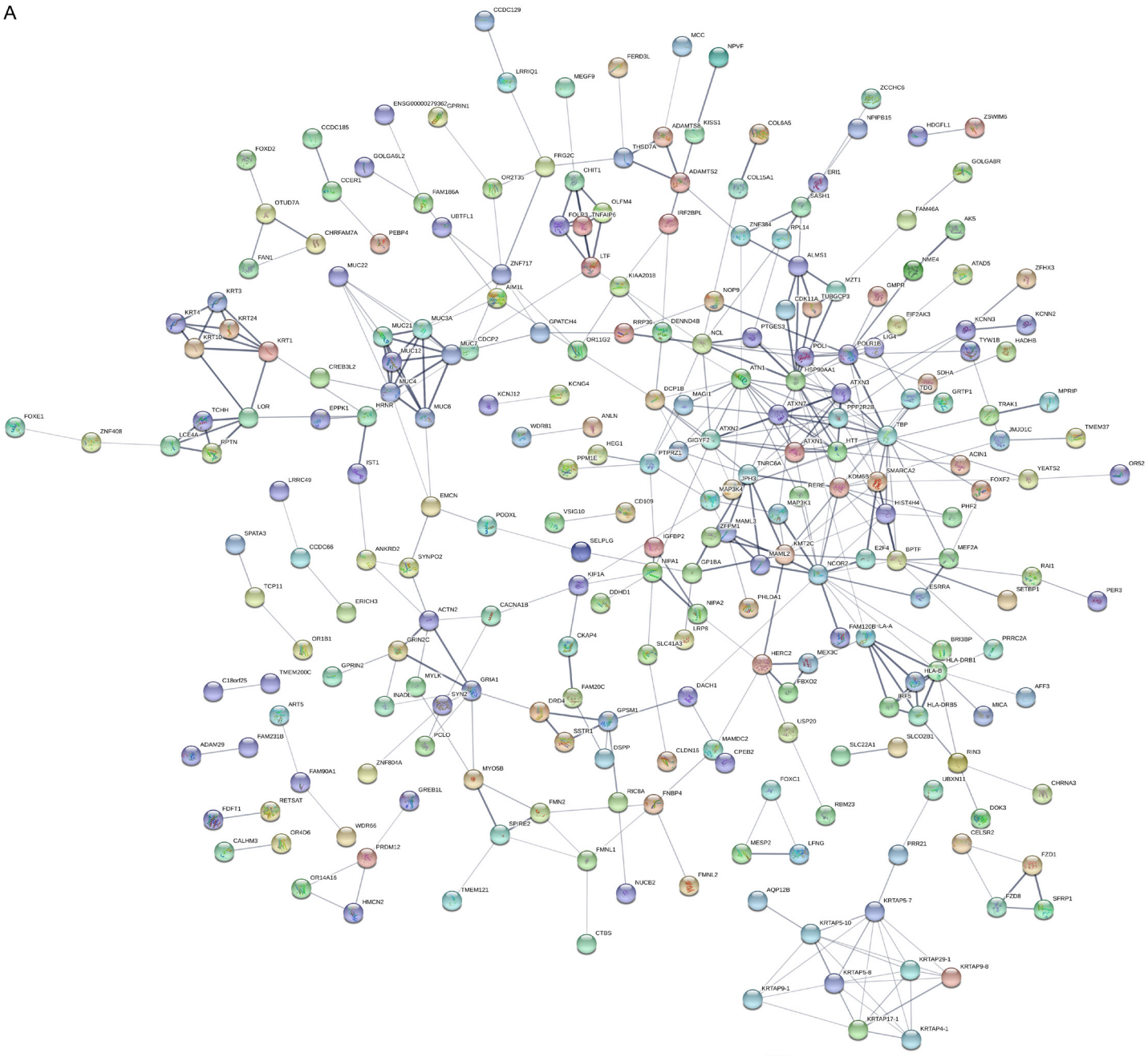
CCDC129
MCC
NPVF
FERD3L
LRRIQ1
MEGF9
ZCCHC6
NPIPB15
HDGFL1
ZSWIM6
ENSG00000279362
GPRIN1
ADAMTS8
KISS1
COL6A5
CCDC185
THSD7A
FOXD2
GOLGA6L2
FRG2C
CHIT1
ADAMTS2
COL15A1
GOLGA8R
CCER1
OR2T35
ERI1
SASH1
FAM186A
OLFM4
FAM46A
OTUD7A
FOXL3
TNFAIP6
IRF2BPL
ZNF384
RPL14
AK5
CHRFAM7A
PEBP4
UBTFL1
ALMS1
NME4
ATAD5
FAN1
ZNF717
LTF
MUC22
KIAA2018
MZT1
GMPR
ZFHX3
AIM1L
NOP9
CDK11A
TUBGCP3
KRT3
KRT4
KRT24
KRT10
KRT1
MUC21
MUC3A
MUC7
MUC12
CDCP2
GPATCH4
RRP36
DENND4B
NCL
PTGES3
POLI
POLR1B
LIG4
EIF2AK3
KCNN3
KCNN2
TYW1B
HADHB
OR11G2
CREB3L2
MUC4
ATN1
HSP90AA1
ATXN3
SDHA
TDG
GRTP1
MPRIP
KCNJ12
KCNG4
DCP1B
MAGI1
ATXN7
PPP2R2B
TRAK1
FOXE1
ZNF408
TCHH
LOR
EPPK1
HRNR
MUC6
WDR81
ANLN
TBP
JMJD1C
TMEM37
LCE4A
RPTN
HEG1
GIGYF2
ATXN2
ATXN1
HTT
PTPRZ1
PPM1E
ACIN1
YEATS2
OR52
IST1
TNRC6A
SMARCA2
KDM6B
JPH3
RERE
FOXF2
LRRC49
MAP3K4
MAP3K1
HIST4H4
PHF2
EMCN
CD109
VSIG10
PODXL
ZFPM1
MAML3
SPATA3
IGFBP2
SELPLG
KMT2C
MAML2
E2F4
BPTF
MEF2A
CCDC66
ANKRD2
SYNPO2
NIPA1
GPI8A
NCOR2
RAI1
KIF1A
ESRRA
SETBP1
PER3
TCP11
DDHD1
NIPA2
PHLDA1
ERICH3
ACTN2
CACNA1B
LRP8
FAM120B
LA-A
OR1B1
GRIN2C
CKAP4
SLC41A3
BRI3BP
PRRC2A
HERC2
MEX3C
HLA-DRB1
GPRIN2
TMEM200C
C18orf25
MYLK
GRIA1
FBXO2
HLA-B
AFF3
INADL
SYN2
FAM20C
DACH1
IRF5
HLA-DRB5
MICA
ART5
DRD4
GPSM1
USP20
ADAM29
FAM231B
PCLO
SSTR1
MAMDC2
SLCO2B1
SLC22A1
RIN3
ZNF804A
DSPP
CLDN16
CPEB2
UBXN11
CHRNA3
MYO5B
FOXC1
FAM90A1
RICBA
FNBP4
RBM23
DOK3
GREB1L
FMN2
RETSAT
FDFT1
SPIRE2
MESP2
LFNG
CELSR2
WDR66
OR4D6
CALHM3
PRDM12
FMNL1
PRR21
FZD1
OR14A16
NUCB2
FMNL2
FZD8
SFRP1
HMCN2
TMEM121
AQP12B
KRTAP5-7
KRTAP5-10
CTBS
KRTAP29-1
KRTAP9-8
KRTAP5-8
KRTAP9-1
KRTAP17-1
KRTAP4-1

B

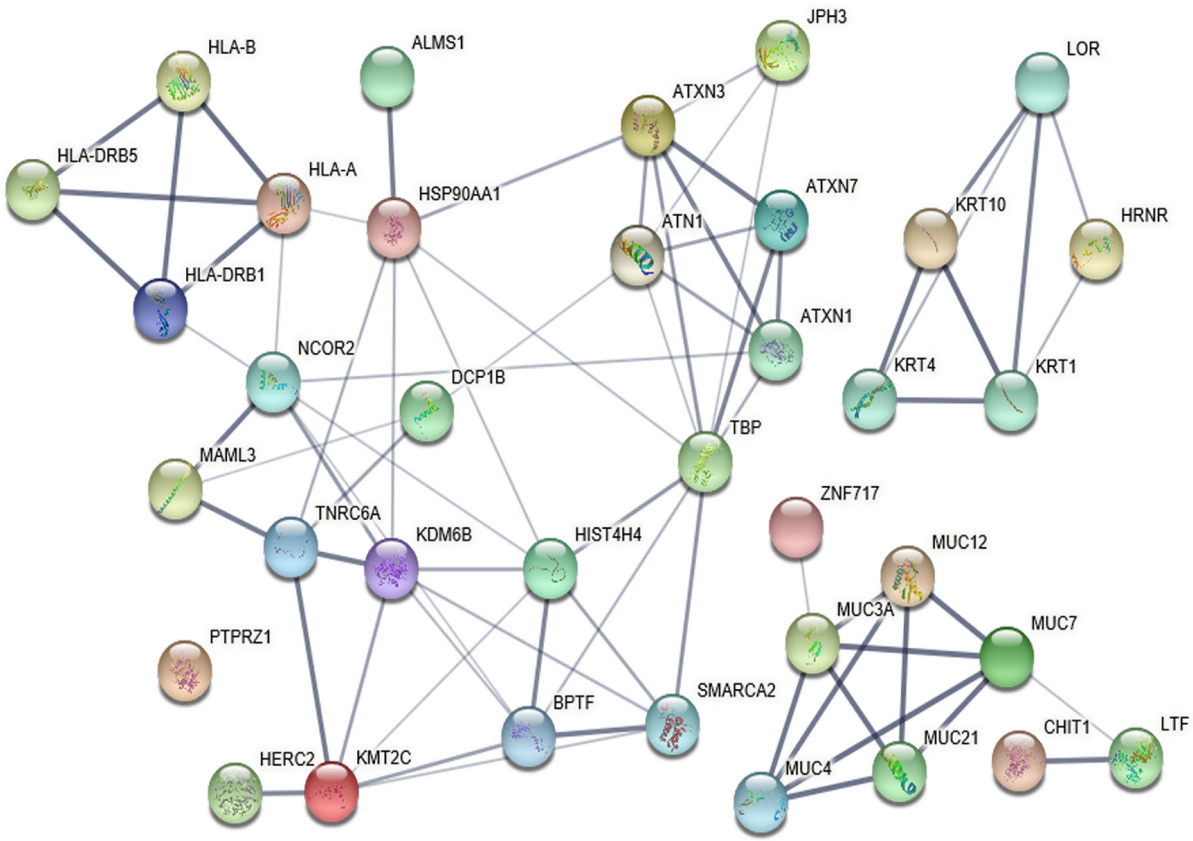

Figure 5. Protein-protein interaction (PPI) networks of mutated genes in case 2 (Y4935). A. The interaction among the mutated genes defined in our study. The larger the radius of the circle of a gene, the more interaction can be seen between the gene and other genes. The width of the line represents the strength of the interaction. B. Top three modules from protein-protein interaction network by Cytoscape analysis.

most common subtype of MDS-LGLL patients and erythroid dysplasia could be observed in all the MDS-LGLL patients. We identified cytogenetic abnormalities in 20% (2/10) of cases.

Similar research has carried by Maciejewski who applied deep NGS for only 36 MDS-associated mutant genes in MDS-TGLL patients to find a coincidence between CHIP and LGL [11]. Based on our research, we detected mutations of myeloid and lymphoid-associated genes including *EZH2, TET2, DNMT3A, TP53* and *ATM*, myeloid-associated genes including *ASXL1, STAG2, FLT3, U2AF1, WT1, CUX1, TIN, SETBP1, SH2B3, CDC25C, KIT, CSF3R, ATG2B, CEBPA, ANKRD26, CBL, DDX41, GATA2* [23] and lymphoid-associated genes including *STAT3, STAT5b, FAT1, DIS3, PAX5, PTEN, TNFAIP3, PTPRT, NOTCH1, and PRDM1.* Driver genes (*ASXL1, STAG2, EZH2* and so on) have been identified that are involved in the pathogenesis of MDS [24]. Mutations of lymphoid-associated genes such as *STAT3, STAT5b, TNFAIP3, PTPRT* were worthy of our attention. *STAT3* mutations were mostly detected in almost 40% of patients with T-LGLL and CLPD-NK [25]. *STAT5b* mutations have also been identified in 5-10% cases [12]. Besides, *TNFAIP3* and *PTPRT* are related to LGLL as reported [26]. Non-synonymous alterations in the *TNFAIP3* tumor suppressor gene were captured in 3 of 39 T-LGLL [26]. Another study report rare genetic triggering of T-LGLL due to mutations in the *PTPRT, BCL-11B, SLIT2* and *NRP1* genes [27]. In our study, *TNFAIP3* mutation was detected in case 2 and PTPRT mutation was detected in case 9, which might further indicate the activation of *JAK/STAT* pathways.

Based on pathologic and immunophenotypic findings, we reported coexistence of MDS and mixed-phenotype LGLL in two cases for the first time. A rare case of the mixed-phenotype LGLL has been reported [17, 28, 29] and possibly caused by persistent antigenic pressure of clonal expansion in Cytotoxic T cells and NK cells alone, together or even inter switchingly [30].

Mutations of J9575M and Y4935 were analyzed by GO pathway enrichment analyses to explore the change of mutations spectrum from MDS phase to MDS-LGLL phase. The enrichment of H3K4 mono-methylation increased, while the genes related to Translocation of ZAP-70 to immunological synapse pathway was significantly less enriched. According to previous study, missense and truncating mutations are frequently found in MDS patients in modifiers of H3K4 methylation [31]. Proper regulation of H3K4me1 has been implicated in HSC self-renewal and in regulating proper differentiation. The translocation of ZAP-70, required in initiating the canonical biochemical signal pathways downstream of the TCR [32], might associate with proliferation of LGLs. Whereas, the observations need be further demonstrated because of small sample size. More cases of MDS-LGLL need to be accumulated for NGS, WES and GO analysis for the further research.

In summary, we described clinicopathological features and mutational profile of MDS-LGLL patients. NGS of MDS-LGLL cases showed 37 myeloid-lymphoid-associated mutated genes. Additionally, we observed an increased enrichment of H3K4 mono-methylation and a decreased enrichment of translocation of ZAP-70 upon the progression from MDS to MDS-LGLL. Up to now, the observations of MDSLGLL are still limited and the pathogenesis is also unclear. Firstly, our study may be helpful for explanation of the validity of immunosuppressive treatment for a subgroup of MDS patients. Secondly, other studies had described a few cases of MDS patients presented a transformation to acute lymphoblastic leukemia (ALL) [33]. We surmised LGL might affect the progression and transformation of MDS. The pathogenesis is complex and we want to go further in terms of mechanisms. Thirdly, we hypothesized that the hematopoietic stem cells (HSCs) of MDS-LGLL patients were abnormal and differentiated dysfunction. We will focus on the inference of LGL and follow up these patients. Accumulation of cases, along with NGS and bioinformatic gene analyses will promote understanding of the underlying mechanisms and treatment of MDS-LGLL in the future.

Acknowledgements

This study was supported by The National Natural Science Foundation of China (82070176, 82070128, 81900132), Guangdong Provincial Science and Technology Projects (2017B020230004), Guangzhou Regenerative Medicine and Health Guangdong Laboratory Projects (2018GZR0201008).

Disclosure of conflict of interest

None.

Address correspondence to: Drs. Xin Du and Jianyu Weng, Department of Hematology, Guangdong Provincial People's Hospital, Guangdong Academy of Medical Sciences, 106 Zhongshan Er Road, Guangzhou 510080, Guangdong, P. R. China. E-mail: xind_gdph2020@163.com; miyadu@hotmail.com (XD); wengjianyu1969@163.com (JYW)

References

[1] Arber DA, Orazi A, Hasserjian R, Thiele J, Borowitz MJ, Le Beau MM, Bloomfield CD, Cazzola M and Vardiman JW. The 2016 revision to the World Health Organization classification of myeloid neoplasms and acute leukemia. Blood 2016; 127: 2391-2405.

[2] Ivy KS and Brent Ferrell P Jr. Disordered immune regulation and its therapeutic targeting in myelodysplastic syndromes. Curr Hematol Malig Rep 2018; 13: 244-255.

[3] Parikh AR, Olnes MJ and Barrett AJ. Immunomodulatory treatment of myelodysplastic syndromes: antithymocyte globulin, cyclosporine, and alemtuzumab. Semin Hematol 2012; 49: 304-311.

[4] Swerdlow SH, Campo E, Pileri SA, Harris NL, Stein H, Siebert R, Advani R, Ghielmini M, Salles GA, Zelenetz AD and Jaffe ES. The 2016 revision of the World Health Organization classification of lymphoid neoplasms. Blood 2016; 127: 2375-2390.

[5] Cheon H, Dziewulska KH, Moosic KB, Olson KC, Gru AA, Feith DJ and Loughran TP. Advances in the diagnosis and treatment of large granular lymphocytic leukemia. Curr Hematol Malig Rep 2020; 15: 103-112.

[6] Lamy T, Moignet A and Loughran TP Jr. LGL leukemia: from pathogenesis to treatment. Blood 2017; 129: 1082-1094.

[7] Moignet A and Lamy T. Latest advances in the diagnosis and treatment of large granular lymphocytic leukemia. Am Soc Clin Oncol Educ Book 2018; 38: 616-625.

[8] Huh YO, Medeiros LJ, Ravandi F, Konoplev S, Jorgensen JL and Miranda RN. T-cell large granular lymphocyte leukemia associated with myelodysplastic syndrome: a clinicopathologic study of nine cases. Am J Clin Pathol 2009; 131: 347-356.

[9] Sauntharajah Y, Molldrem JL, Rivera M, Williams A, Stetler-Stevenson M, Sorbara L, Young NS and Barrett JA. Coincident myelodysplastic syndrome and T-cell large granular lymphocytic disease: clinical and pathophysiological features. Br J Haematol 2001; 112: 195-200.

[10] Bassan R, Marini B, Allavena P, Pirelli A and Barbui T. RAEB in a patient with chronic granulated T-lymphocytosis. Br J Haematol 1987; 65: 503-504.

[11] Durrani J, Awada H, Kishtagari A, Visconte V, Kerr C, Adema V, Nagata Y, Kuzmanovic T, Hong S, Patel B, Nazha A, Lichtin A, Mukherjee S, Sauntharajah Y, Carraway H, Sekeres M and Maciejewski JP. Large granular lymphocytic leukemia coexists with myeloid clones and myelodysplastic syndrome. Leukemia 2020; 34: 957-962.

[12] Hematopathology. 2020.

[13] Bruggemann M, White H, Gaulard P, Garcia-Sanz R, Gameiro P, Oeschger S, Jasani B, Ott M, Delsol G, Orfao A, Tiemann M, Herbst H, Langerak AW, Spaargaren M, Moreau E, Groenen PJ, Sambade C, Foroni L, Carter GI, Hummel M, Bastard C, Davi F, Delfau-Larue MH, Kneba M, van Dongen JJ, Beldjord K and Molina TJ. Powerful strategy for polymerase chain reaction-based clonality assessment in T-cell malignancies report of the BIOMED-2 concerted Action BHM4 CT98-3936. Leukemia 2007; 21: 215-221.

[14] Montalban-Bravo G and Garcia-Manero G. Myelodysplastic syndromes: 2018 update on diagnosis, risk-stratification and management. Am J Hematol 2018; 93: 129-147.

[15] Greenberg PL, Tuechler H, Schanz J, Sanz G, Garcia-Manero G, Sole F, Bennett JM, Bowen D, Fenaux P, Dreyfus F, Kantarjian H, Kuendgen A, Levis A, Malcovati L, Cazzola M, Cermak J, Fonatsch C, Le Beau MM, Slovak ML, Krieger O, Luebbert M, Maciejewski J, Magalhaes SM, Miyazaki Y, Pfeilstocker M, Sekeres M, Sperr WR, Stauder R, Tauro S, Valent P, Vallespi T, van de Loosdrecht AA, Germing U and Haase D. Revised international prognostic scoring system for myelodysplastic syndromes. Blood 2012; 120: 2454-2465.

[16] Shi M, He R, Feldman AL, Viswanatha DS, Jevremovic D, Chen D and Morice WG. STAT3 mutation and its clinical and histopathologic correlation in T-cell large granular lymphocytic leukemia. Hum Pathol 2018; 73: 74-81.

[17] Neff JL, Rangan A, Jevremovic D, Nguyen PL, Chiu A, Go RS, Chen D, Morice WG and Shi M. Mixed-phenotype large granular lymphocytic leukemia: a rare subtype in the large granular lymphocytic leukemia spectrum. Hum Pathol 2018; 81: 96-104.

[18] Wang SA and Hasserjian RP. T- and NK-Cell Lymphocytosis. Diagnosis of Blood and Bone Marrow Disorders. 2018. pp. 281-328.

[19] Singleton TP, Yin B, Teferra A and Mao JZ. Spectrum of clonal large granular lymphocytes (LGLs) of alphabeta T cells: T-cell clones of undetermined significance, T-cell LGL leukemias,

and T-cell immunoclones. Am J Clin Pathol 2015; 144: 137-144.
[20] Zhu Y, Gao Q, Hu J, Liu X, Guan D and Zhang F. Clinical features and treatment outcomes in patients with T-cell large granular lymphocytic leukemia: a single-institution experience. Leuk Res 2020; 90: 106299.
[21] Zhang X, Sokol L, Bennett JM, Moscinski LC, List A and Zhang L. T-cell large granular lymphocyte proliferation in myelodysplastic syndromes: clinicopathological features and prognostic significance. Leuk Res 2016; 43: 18-23.
[22] Komrokji RS, Ali NA, Sallman D, Padron E, Lancet J, Sokol L, Varnadoe C, Burnette PK and List A. Characterization of myelodysplastic syndromes (MDS) with T-cell large granular lymphocyte proliferations (LGL). Leukemia 2020; 34: 3097-3099.
[23] Li B, Liu J, Xu Z, Qin T, Shi Z, Song Z, Huang H, Fang L, Zhang H, Pan L, Hu N, Qu S, Zhang Y, Huang G and Xiao Z. The usefulness of mutational data on prognosis of myelodysplastic syndromes: alone or incorporated into the IPSS-R? Br J Haematol 2018; 183: 815-819.
[24] Ogawa S. Genetics of MDS. Blood 2019; 133: 1049-1059.
[25] Jerez A, Clemente MJ, Makishima H, Koskela H, Leblanc F, Peng Ng K, Olson T, Przychodzen B, Afable M, Gomez-Segui I, Guinta K, Durkin L, Hsi ED, McGraw K, Zhang D, Wlodarski MW, Porkka K, Sekeres MA, List A, Mustjoki S, Loughran TP and Maciejewski JP. STAT3 mutations unify the pathogenesis of chronic lymphoproliferative disorders of NK cells and T-cell large granular lymphocyte leukemia. Blood 2012; 120: 3048-3057.
[26] Johansson P, Bergmann A, Rahmann S, Wohlers I, Scholtysik R, Przekopowitz M, Seifert M, Tschurtschenthaler G, Webersinke G, Jager U, Siebert R, Klein-Hitpass L, Duhrsen U, Durig J and Kuppers R. Recurrent alterations of TNFAIP3 (A20) in T-cell large granular lymphocytic leukemia. Int J Cancer 2016; 138: 121-124.
[27] Andersson EI, Rajala HL, Eldfors S, Ellonen P, Olson T, Jerez A, Clemente MJ, Kallioniemi O, Porkka K, Heckman C, Loughran TP Jr, Maciejewski JP and Mustjoki S. Novel somatic mutations in large granular lymphocytic leukemia affecting the STAT-pathway and T-cell activation. Blood Cancer J 2013; 3: e168.
[28] Sandberg Y, Dezentje VO, Szuhai K, van Houte AJ, Tielemans D, Wolvers-Tettero IL, van Dongen JJ, van der Griend R and Langerak AW. Clonal T- and natural killer-cell large granular lymphocyte proliferations in a single patient established by array-based comparative genomic hybridization analysis. Leukemia 2006; 20: 2212-2214.
[29] Yan Y, Olson TL, Nyland SB, Feith DJ and Loughran TP Jr. Emergence of a STAT3 mutated NK clone in LGL leukemia. Leuk Res Rep 2015; 4: 4-7.
[30] Gattazzo C, Teramo A, Passeri F, De March E, Carraro S, Trimarco V, Frezzato F, Berno T, Barila G, Martini V, Piazza F, Trentin L, Facco M, Semenzato G and Zambello R. Detection of monoclonal T populations in patients with KIR-restricted chronic lymphoproliferative disorder of NK cells. Haematologica 2014; 99: 1826-1833.
[31] Heuser M, Yun H and Thol F. Epigenetics in myelodysplastic syndromes. Semin Cancer Biol 2018; 51: 170-179.
[32] Au-Yeung BB, Shah NH, Shen L and Weiss A. ZAP-70 in signaling, biology, and disease. Annu Rev Immunol 2018; 36: 127-156.
[33] Martins F, Kruszewski M, Scarpelli I, Schoumans J, Spertini O, Lubbert M and Blum S. Characterization of myelodysplastic syndromes progressing to acute lymphoblastic leukemia. Ann Hematol 2021; 100: 63-78.

Table S1. The panel of 114 genes detected by Next generation sequencing (NGS)

ABL1	ETV6	RBBP6	MYD88	GATA2	CXCR4	CCR4
ACD	TERC	RELN	NF1	GATA3	DDX3x	cD79B
ANKRD26	TERT	RHOA	NOTCH1	HNRNPK	DDx41	cDC25C
ASXL1	TET2	RUNX1	NOTCH2	ID3	DIS3	CDKN1B
ATG2B	TNFAIP3	SETBP1	NPM1	IDH1	DNM2	CDKN2A
ATM	TP53	SETD2	NRAS	IDH2	DNMT3A	CEBPA
B2M	TPMT	SF1	PAX5	IKZF1	DNMT3B	CREBBP
BCOR	TRAF3	SF3A1	PDS5B	IL7R	ECT2L	CSF3R
BCORL1	U2AF1	SF3B1	PHF6	JAK1	EED	cUX1
BIRC3	U2AF2	SH2B3	PIGA	JAK2	EP300	MAPK1
BRAF	wHSC1	SMC1A	PLCG1	JAK3	ETNK1	KMT2D
CALR	wT1	SMC3	PRKCB	KDM6A	EZH2	MPL
CARD11	xPO1	SRP72	PRPF40B	KIT	FAM46C	MYC
CBL	ZMYM3	SRSF2	PRPS1	KMT2A	BRINP3	FBxW7
CCND1	ZRSR2	STAG2	PTEN	KRAS	FAT1	FGFR3
CCND3	ARID1A	STAT3	PTPN11	RAD21	sUz12	FLT3
GATA1	RB1					

Table S2. Whole-exome sequencing (WES) analysis of J9575M and Y4935

Sample	J9575M	Y4935
CDS	22432	22418
Synonymous_SNP	11415	11432
Missense_SNP	10689	10694
Stopgain	77	73
Stoploss	9	9
Unknow	248	216
Intronic	108162	106961
UTR3	5382	5377
UTR5	3091	3131
Splicing	63	64
ncRNA_exonic	3148	3204
ncRNA_intronic	8186	8010
ncRNA_splicing	13	12
Upstream	4001	4041
Downstream	1919	1907
Intergenic	51161	51178
Total	207811	206562

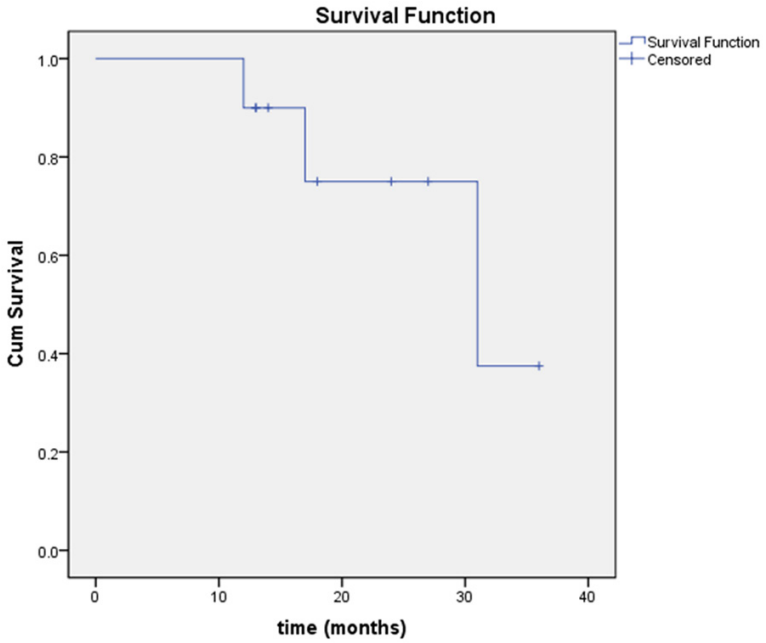

Figure S1. Overall survival of Myelodysplastic syndromes concurrent with large granular lymphocytic leukemia (MDS-LGLL) patients by Kaplan-Meier analysis.